

# Feasible platform to study negative temperatures

R. J. de Assis,<sup>1</sup> C. J. Villas-Boas,<sup>2</sup> and N. G. de Almeida<sup>1</sup>

<sup>1</sup>*Instituto de Física, Universidade Federal de Goiás, 74.001-970, Goiânia - GO, Brazil*

<sup>2</sup>*Departamento de Física, Universidade Federal de São Carlos, 13565-905, São Carlos, São Paulo, Brazil*

We afford an experimentally feasible platform to study Boltzmann negative temperatures. Our proposal takes advantage of well-known techniques of engineering Hamiltonian to achieve steady states with highly controllable population inversion. Our model is completely general and can be applied in a number of contexts, such as trapped ions, cavity-QED, quantum dot coupled to optical cavities, circuit-QED, and so on. To exemplify, we use Hamiltonian models currently used in optical cavities and trapped ion domain, where the level of precision achieved the control of the freedom degrees of a single atom inside a cavity/trapped ion. We show several interesting effects such as absence of thermalization between systems with inverted population and cooling by heating in these unconventional systems.

PACS numbers: 05.30.-d, 05.20.-y, 05.70.Ln

## I. INTRODUCTION

Negative temperature  $T$  is associated with systems with a bounded energy spectrum for which  $1/T = (\partial S/\partial E)_V < 0$ , where  $S$  is the Boltzmann entropy. In general, negative temperatures can be observed in the population-inverted states, which can be achieved by injecting energy into these systems in the right way. The concept of negative temperature was proposed in the early 1950s [1, 2], and since then has been discussed in a number of papers [3–11]. Very recently, negative temperature was experimentally observed using ultracold quantum gases [12]. The experiment in [12] triggered a vivid debate regarding the existence of negative absolute temperatures, with the opponents claiming that negative absolute temperature should not exist if the "right" (Gibbs) entropy is used [13–16] while those in favor of Boltzmann entropy claiming that negative temperatures not only exist as it is necessary to explain systems presenting population inversion [17–20]. Although this debate is far from a consensus, it seems to indicate that while Boltzmann's entropy is adequate to describe the canonical ensemble in the thermodynamical limit, Gibbs's entropy should be used to describe the micro-canonical ensemble [15, 16] and, at least tentatively, systems with finite dimension [14]. Anyway, it is not our aim to enter in the debate on what is the right absolute temperature, or, equivalently, the right entropy. Rather, here we take a pragmatic approach of considering Boltzmann entropy, which leads to temperatures that can be negative for systems with inverted population.

Taking advantage of well-known techniques of Hamiltonian engineering [21, 22], in this paper we afford a platform experimentally feasible in several contexts, as for example quantum circuits, cavity QED and trapped ions. Particularly, here we explore a model in the context of optical cavities and trapped ions, in which the extraordinary level of precision reaches the control of individual atoms, in order to engineer systems dis-

playing negative Boltzmann temperature. To our aim, we work with an ion trapped in a harmonic potential pumped by a laser field to build steady states of the excited ionic levels, therefore with inverted population. Similar inverted population can also be achieved with single trapped atom inside an optical cavity, by properly engineering the atom-cavity mode interaction with the help of external laser fields as done in [23]. Within our model, we are able to provide the range of values that negative temperatures can be observed. After that, we study thermalization of two systems when one of them, displaying negative temperatures, is put in contact with a second one. We show that steady states of systems involving negative temperatures can show very surprising behaviors, as for example absence of thermalization with other systems.

## II. MODEL

To our purpose, we make use of the so-called generalized anti-Jaynes-Cummings model (AJCM) [24], which, can be derived as follows. Consider a trapped two-level ion whose transition frequency between its excited and ground states is  $\omega_0$  and the trap frequency is  $\nu$ . The quantum of vibrational energy of the center of mass of the ion is described by  $a^\dagger a$ . In the Schrödinger picture, the Hamiltonian that describes such a system is  $H = H_f + H_a + H_{int}(t)$ , with  $H_f = \nu a^\dagger a$ ,  $H_a = \omega_0 \sigma_z/2$

$$H_{int}(t) = \frac{\Omega}{2} \left[ \sigma_- e^{i(k\hat{x} + \omega_L t)} + \sigma_+ e^{-i(k\hat{x} + \omega_L t)} \right], \quad (\text{II.1})$$

where  $\hbar = 1$  and the Rabi frequency (ion-laser coupling)  $\Omega$  is much smaller than the bosonic ( $\nu$ ) and atomic transition ( $\omega_0$ ) frequencies;  $\sigma_+$  ( $\sigma_-$ ) is the raising (lowering) Pauli operator for a two-level ionic system,  $\sigma_z = \sigma_+ \sigma_- - \sigma_- \sigma_+$ ,  $a$  ( $a^\dagger$ ) is the annihilation (creation) operator in the Fock space for the bosonic mode, and  $\omega_L$  is the frequency of the driving laser. Here  $k\hat{x} = \eta_L(a + a^\dagger)$ ,

and  $\eta_L = k/\sqrt{2mv}$  is the Lamb-Dicke parameter [24]. Working in the limit  $\eta_L \ll 1$  and applying the rotating-wave approximation, the Hamiltonian  $H_{int}(t)$  in the interaction picture has the time-independent form

$$H_I = g_k \left( \sigma_- a^k + \sigma_+ a^{\dagger k} \right), \quad (\text{II.2})$$

where, by adjusting the frequency  $\omega_L$  such that  $\delta = \omega_L - \omega_0 = kv$  on resonance with the two-level ion, we can have, for instance, interactions i) carrier ( $k = 0$ ,  $g_0 = \Omega/2$ ) ii) the first ( $k = 1$ ,  $g_1 = i\Omega\eta_L/2$ ) and iii) second ( $k = 2$ ,  $g_2 = -i\eta_L^2\Omega/4$ ) blue sideband, and so on [25, 26]. Note that, as we are working in the  $\eta \ll 1$  limit, the nonlinear dependence of the coupling with  $a^\dagger a$  can be neglected [26]. This Hamiltonian experimentally model a number of systems, as for example trapped ions [24, 27], a two-level (TL) atom pumped by a classical electromagnetic field (EM) and interacting with a quantized mode of a EM [28], a coupling between spin and nanomechanical resonator [29] or either a TL neutral atom in a dipole trap or a TL ion in a harmonic trap [30–32]. The dynamics of this model for weak system-reservoir coupling can be described by the master equation formalism, which for the Hamiltonian (Eq. (II.2)) reads

$$\begin{aligned} \frac{\partial \rho}{\partial t} = & -i[H_I, \rho] + \kappa \left( n_f + 1 \right) \mathcal{D}[a]\rho + \kappa n_f \mathcal{D}[a^\dagger]\rho \\ & + \gamma \left( n_a + 1 \right) \mathcal{D}[\sigma_-]\rho + \gamma n_a \mathcal{D}[\sigma_+]\rho \end{aligned} \quad (\text{II.3})$$

where  $\kappa$  and  $\gamma$  are the spontaneous emission rates for the vibrational mode and atom, respectively,  $n_f$  ( $n_a$ ) is the average photon number for the vibrational mode (atom) reservoir, and  $D[A]\rho \equiv 2A\rho A^\dagger - A^\dagger A\rho - \rho A^\dagger A$ .

Next, we solve numerically Eq. (II.3) to obtain the steady state of the system at  $t \rightarrow \infty$  by imposing  $\partial\rho/\partial t = 0$  and thus to calculate the corresponding thermodynamic properties. We note that for solving numerically this system we must truncate the infinite Fock basis of the bosonic fields somewhere, which depend on the mean number of excitations in the bosonic field (vibrational mode). To proceed a numerical study of Eq. (II.3) [33], we assume both reservoirs with the same average number of thermal photons, i.e.,  $n_f = n_a = n$ . Also, as we are particularly interested on the TL system, whose asymptotic behavior can present inverted population, we trace over the bosonic field variables. Next, we use the master Eq. (II.3) to investigate negative temperatures for a range of parameters represented by the cooperativity  $C_k = g_k^2/\gamma\kappa$ . The cooperativity is the experimentally relevant parameter and depends on the physical context. For instance, in the context of optical cavities it was experimentally realized up to  $C \sim 35$  [30].

It is important to mention some differences and similarities between our model and the system used in [12].

As in [12], we use external fields to engineer an effective Hamiltonian which drives the system to a stationary regime with population inversion. In the experiment with cold atoms in optical lattices described in [12], via Feshbach's resonance, an effective interaction is engineered to prepare a steady state with negative temperature, that is, starting from a state without population inversion, the system reaches a state with population inversion for sufficiently long times. However, it is important to note that the relevant dissipative mechanics considered in [12] are sufficiently weak such that they can be disregarded in that experiment, allowing to treat the atomic ensemble as an isolated system. In our model, the dissipation of the atom is taken into account and it is responsible for destroying the state with population inversion. However, the engineered effective interaction with the bosonic mode plus its dissipation result in an effective engineered reservoir which leads the system to a state with inverted population. Thus, as we take into account the ionic dissipation in our model, here we have a competition between the action of the natural dissipation of the ion (spontaneous emission) and the action of the engineered interaction.

### III. PRODUCING STEADY STATES WITH NEGATIVE TEMPERATURES

Let us begin by investigating how the energy and the corresponding effective temperature of the TL system varies with the cooperativity. As said before, we are interested in the steady state, such that we consider the asymptotic limit  $t \rightarrow \infty$  by imposing  $\partial\rho/\partial t = 0$  for  $k = 0, 1, 2, 3$ . In Figs. III.1(a-f), where the cooperativity parameter is displayed in logarithmic scale for clarity, we have considered the environments with average thermal photons  $n = 0, 0.5$ , and  $2.0$ . From Figs. III.1(a,c,e) we see that, except for  $k = 0$  (solid black line), all steady states end with inverted population  $\langle \sigma_z \rangle > 0$ , thus leading to negative temperatures, as shown in Figs. III.1(b,d,f), where the rescaled temperature  $k_B T/\omega_0$  versus cooperativity is shown. Here  $T$  was obtained through  $T = 1/k_B (dS_a/d\langle H_a \rangle)$ , where  $S_a$  is the von Neumann entropy to the ion. Note that the role of nonlinearity is to populate the excited state, thus enhancing the inverted population: the greater  $k$ , the greater the positive average  $\langle \sigma_z \rangle$ , which is also reflected in the negative temperature. It is interesting to note that inverted population can be obtained with small values of cooperativity simply increasing the nonlinearity of the AJCM. Also, note that the bosonic and atomic environments slightly suppress the inversion of population, Figs. III.1(a,c,e), thus avoiding to reach hotter negative temperatures for the TL system. From Figs. III.1(b,d,f) we can see that negative temperatures approach to 0K to all  $k = 1, 2, 3$  and for sufficiently high values of the coop-

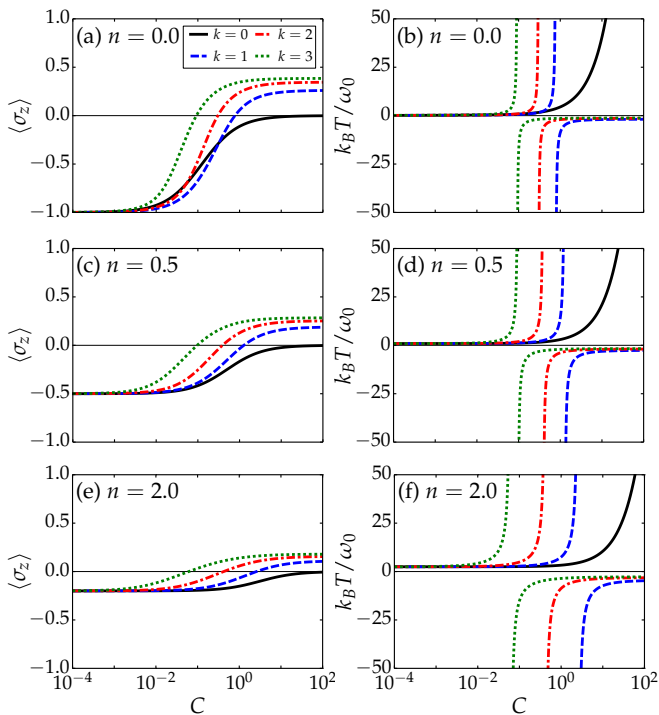


Figure III.1: Atom scaled average energy  $\langle \sigma_z \rangle$  versus cooperativity  $C$ , Figs. (a,c,e), and its scaled effective temperature  $k_B T / \omega_0$  versus cooperativity  $C$ , Figs. (b,d,f). The environment thermal photon averages are  $n = 0.0, 0.5$  and  $2.0$ , respectively. The Hamiltonian models are  $k = 0$  (solid black line),  $k = 1$ , (dashed blue line),  $k = 2$  (dot-dashed red line) and  $k = 3$  (dotted green line). Inverted population occurs for all  $k$  except for  $k = 0$ . Here we used  $\gamma = \kappa$ .

erativity. A numerical inspection shows us that negative temperatures *only* occur for  $C \gtrsim 0.65$ .

#### IV. NEGATIVE TEMPERATURES AND COUPLED SYSTEMS

Here we show how our platform provides an excellent tool for studying thermalization of two coupled systems and how to control the heating or cooling of both systems through cooperativity. Since systems presenting inverted population is hotter than other systems with positive temperatures [34], it is interesting to understand what happens when these *hotter than hot* [35] systems are coupled to each other. Let us consider a two-level atom (A) coupled to another one (B) through a simple exchange interaction  $H_N = \lambda(\sigma_+^A \sigma_-^B + \sigma_-^A \sigma_+^B)$ , which is the usual interaction resulting, for example, of a collision process [36]. The atom A is coupled to a quantum bosonic mode through the effective AJCM Eq. (II.2) and interacts via  $H_N$  with atom B. For simplicity, we assume the vibrational mode, the atom A, and the atom B decaying at the same rate ( $\gamma_A = \gamma_B = \kappa = \gamma$ ).

To study thermalization in these systems, we trace out the degrees of freedom of the bosonic mode for each model  $k = 0, 1, 2$  and  $3$  separately. The case  $k = 0$ , although presenting no population inversion, is considered here only for the effect of comparing thermalization to both atoms A and B.

In Figs. IV.1 we show the average energy for each atom *versus* cooperativity, Figs. IV.1(a,c,e), and the scaled effective temperature (for each atom) *versus* cooperativity, Figs. IV.1(b,d,f), for  $k = 0$  considering the environment photon averages  $n_f = n_a^A = n_a^B = n = 0, 0.5$  and  $2.0$ . As seen from these figures, the populations is not inverted. Also, for  $\lambda = 3\gamma$ , from a certain value of the cooperativity,  $C \gtrsim 8$ , as the energy is not the same for both atoms, Figs. IV.1(a,c,e), the effective temperature, Fig. IV.1(b,d,f), also will be not the same, thus indicating that for  $C \gtrsim 8$  there will be no thermalization. As indicated by our numerical simulation, not shown, the greater  $\lambda$ , the greater the cooperativity required for the atom-atom system to fail to present thermalization. The effect of increasing the environment temperature is to produce steady states with higher temperatures, without producing population inversion.

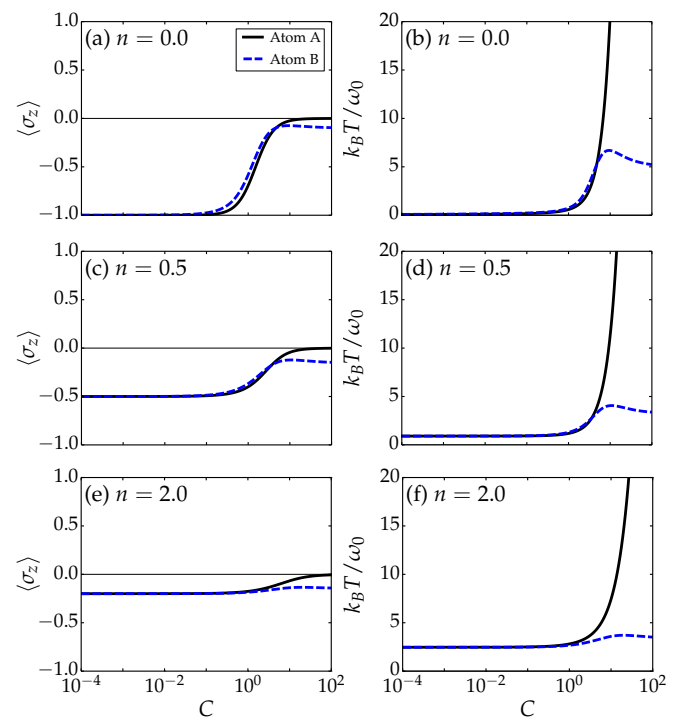


Figure IV.1: Atom scaled average energy  $\langle \sigma_z \rangle$  versus cooperativity, Figs. (a,c,e), and its scaled effective temperature  $k_B T / \omega_0$  versus cooperativity, Figs. (b,d,f), for  $k = 0$ . The environment thermal photon averages are  $n = 0.0, 0.5$ , and  $2.0$ , respectively. Curves for atom A (B) is indicated by solid black (blue dashed) line. Here we used  $\lambda = 3\gamma$  and  $\gamma = \gamma_A = \gamma_B = \kappa$ .

In Fig. IV.2 we show the average energy *versus* cooperativity, Figs. IV.2(a,c,e), and the scaled effective tem-

perature *versus* cooperativity, Figs. IV.2(b,d,f), for  $k = 1$  considering the environment thermal photon averages  $n = 0, 0.5$ , and  $2.0$ . The behavior of these curves, although similar to those in Figs. IV.1(a-f), now show that atom A presents population inversion from  $C \gtrsim 3.5$  different from atom B which always has positive temperatures (for  $\lambda = 3\gamma$ ). Also, for a certain value of  $C$  the energies of atoms A and B are not the same, thus indicating that there will be no thermalization. Here, different from  $k = 0$ , the effect of increasing the environment temperature is to produce steady states with lower negative temperatures. In other words, the positive reservoir tends to lowering the negative temperature of atom A. Another surprising effect is that temperature does not increase monotonically with cooperativity. This effect can be better appreciated looking to the atom B curve in Figs. IV.2(b): by increasing the cooperativity, the temperature of atom B, as given by the dashed blue line, first increase until  $C \approx 4.5$  attaining its maximum, and then decays to zero for large values of the cooperativity.

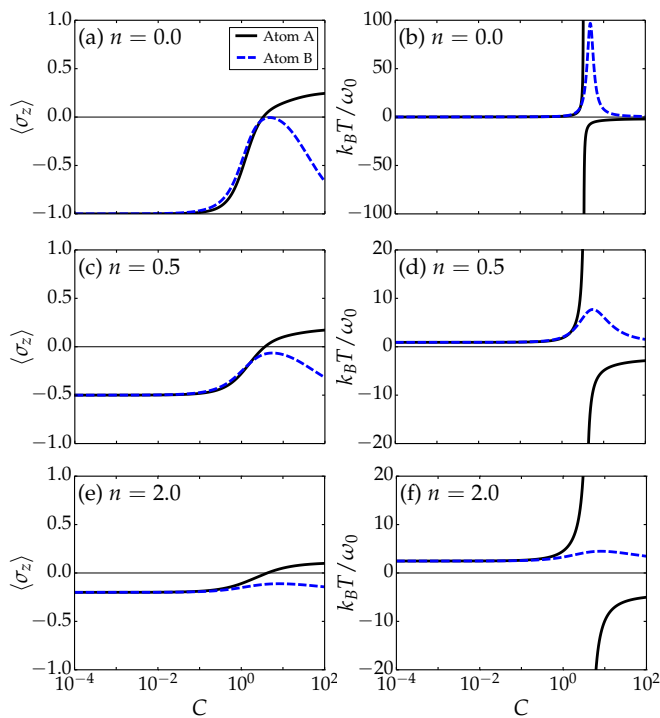


Figure IV.2: Scaled average energy  $\langle \sigma_z \rangle$  *versus* cooperativity, Figs. (a,c,e), and scaled effective temperature  $k_B T / \omega_0$  *versus* cooperativity, Figs. (b,d,f), for  $k = 1$ . The environment thermal photon averages are  $n = 0.0, 0.5$ , and  $2.0$ , respectively. Curves for atom A (B) is indicated by solid black (blue dashed) line. Here we used  $\lambda = 3\gamma$  and  $\gamma = \gamma_A = \gamma_B = \kappa$ . A similar behavior can be seen for models  $k = 2, 3$ .

The models  $k = 2, 3$  presents a similar pattern and will not be shown here: atom B, which is coupled only to atom A, never inverts its population, but cannot be heated arbitrarily, since its temperature reaches a maximum.

Otherwise, atom A, which is coupled both to atom B and to a bosonic mode, is the one that has its population inverted, being this population (and so its negative temperature) diminished when the temperature of the environment reservoir is increased (from  $n = 0$  to  $2.0$ ). Also, the atomic steady states do not thermalize neither with each other nor with the environment.

Now, let us recall that the cooperativity parameter comprehends the coupling between ion A and its vibrational mode as well as the ion A decay rate and the vibrational mode damping through  $C_k = g_k^2 / \gamma_A \kappa$ . Thus, it is also interesting to study how the scaled average energy and the effective temperature behaves when varying the strength coupling  $\lambda$  between atoms A and B, and also asking if it is possible to have thermalization between them. In Fig. IV.3(a-f) and IV.4(a-f) we show the scaled average internal atom energy  $\langle \sigma_z \rangle$  and the effective temperature *versus* the scaled strength coupling  $\lambda / \gamma$  for  $k = 0, 1, 2$ , and  $3$  considering the environment thermal photon averages  $n = 0, 0.5$ , and  $2.0$ . Note from Figs. IV.3(a,c,e) that for  $k = 0$  the populations of atoms A and B are not inverted. Nevertheless, atom B presents an interesting behavior: when the rate  $\lambda / \gamma$  is increased, its population increases until reaching a maximum, and then starts to decrease. On the other hand, atom A population always decrease, until its population becomes equal to that of atom B, when thermalization between atoms A and B thus occurs, see Figs. IV.3(b,d,f), for sufficiently high values of the rate  $\lambda / \gamma$ . Also it is important to note that thermalization between atoms A and B may occur at different temperatures to that of their environments, as can be seen from Figs. IV.3(b,d,f), where the environment has temperatures corresponding to  $n = 0, 0.5$  and  $2.0$ .

In Figs. IV.4(a-f) we now study the model  $k = 1$ . Now, different from Fig. IV.3, both atoms can present negative temperatures. Note that atom B energy increases until crossing the zero energy line, thus inverting its population and acquiring negative temperature, and then starts to decrease until its energy crosses back the zero energy line, acquiring positive temperature. On the contrary, atom A, which starts with inverted population, diminishes its internal energy until crossing the zero line energy, acquiring a positive temperature for sufficiently high value of the rate  $\lambda / \gamma$ . Also, as in the previous case, for sufficiently high values of the rate  $\lambda / \gamma$  both atoms A and B thermalize with each other, although not thermalizing with their environment. It is interesting to note that atom A and B *can thermalize even at negative temperatures*, as is better seen in Figs. IV.4(a-d). The role of the atoms A and B environments is to diminish population inversion, see the blue-dash line in Figs. IV.4(a,c,e), and thus the negative temperature effect. For the parameters used here, the negative temperature of atom B, blue-dash line, is completely suppressed at a temperature corresponding to an average thermal photon

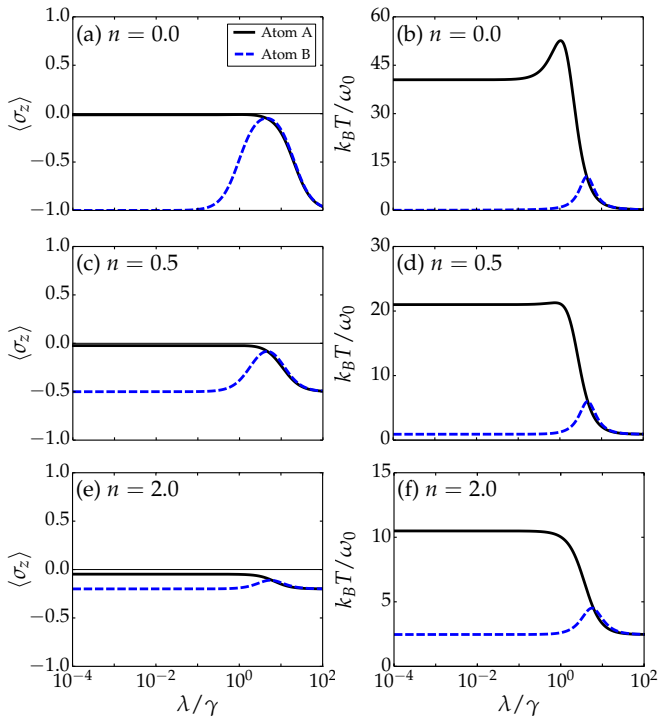


Figure IV.3: Atom scaled average energy  $\langle \sigma_z \rangle$  versus scaled atom-atom coupling ( $\lambda/\gamma$ ), Figs. (a,c,e), and its scaled effective temperature  $k_B T/\omega_0$  versus  $\lambda/\gamma$ , Figs. (b,d,f), for  $k = 0$ . The environment thermal photon averages are  $n = 0.0, 0.5$ , and  $2.0$ , respectively. Curves for atom A (B) is indicated by solid black (blue dashed) line. Here we used  $g_k = \sqrt{10}\gamma$ , and  $\gamma = \gamma_A = \gamma_B = \kappa$ .

$n = 2.0$ .

Figs. IV.5 (a-f) now take into account the Hamiltonian model  $k = 2$ . The same pattern is observed, as in the previous Figs. (IV.3-IV.4): the stronger the nonlinearity of the Hamiltonian model, the higher the population inversion obtained for both atoms. Now the maximum environment temperature for both atoms is not enough to completely suppress negative temperature for atom B, as can clearly be seen from Fig. IV.5(e,f). Also, thermalization between atoms A and B may be seen even for negative temperatures for certain values of the rate  $\lambda/\gamma$  and, by increasing this rate a bit, both atoms acquire positive temperature, where thermalization also occurs. Our numerical analyses show that the same qualitative behavior is seen for the model  $k = 3$  (not shown).

## V. UNCONVENTIONAL COOLING BY HEATING (CBH)

Now let us analyze the case where both the bosonic mode and atoms A and B are surrounded by an environment at the same temperature  $T$  characterized by an average number  $n$  of thermal photons. We again assume here that both atoms decay with the same rate

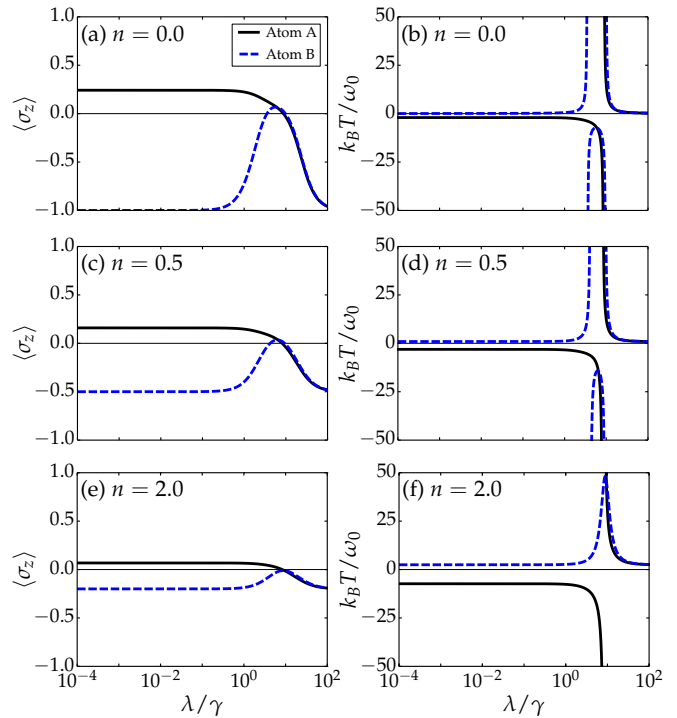


Figure IV.4: Scaled average energy  $\langle \sigma_z \rangle$  versus scaled atom-atom coupling ( $\lambda/\gamma$ ), Figs. (a,c,e), and scaled effective temperature  $k_B T/\omega_0$  versus  $\lambda/\gamma$ , Figs. (b,d,f), for  $k = 1$ . The environment thermal photon averages are  $n_{th} = 0.0, 0.5$ , and  $2.0$ , respectively. Curves for atom A (B) is indicated by solid black (blue dashed) line. Here we used  $g_k = \sqrt{10}\gamma$  and  $\gamma = \gamma_A = \gamma_B = \kappa$ .

$\gamma_A = \gamma_B = \kappa = \gamma$  and interact with each other through the natural coupling  $H_N = \lambda(\sigma_+^A \sigma_-^B + \sigma_-^A \sigma_+^B)$ . The cooperativity is fixed at  $C = 10$ . Meanwhile, atom A is pumped with a laser leading to the effective Hamiltonian Eq. (II.2) between atom A and the quantized vibrational mode. Since in this case the interaction considered between the two atoms is the usual (or natural) one, one could expect thermalization between the atoms, which would eventually prevent CBH [25], at least in conventional systems with positive temperatures. Actually, as discussed, e.g. in Refs. [25], to achieve CBH in conventional systems (positive temperatures) it is necessary to engineer a Hamiltonian whose major contribution is due to counter-rotating terms. This is because two systems, modeled by the usual Hamiltonians as given by matter-radiation interaction, generally thermalize with their environment and, when in contact, thermalize with each other. However, as we saw in Figs. (IV.1) and (IV.2), the steady state of atom A can display negative temperature, and thus an *unconventional* CBH with systems presenting negative temperatures can indeed occur, despite the coupling being a natural (not engineered) one. To see this, in Fig. (V.1)(a-h) we show the scaled average internal atom energy and the scaled effective temperature

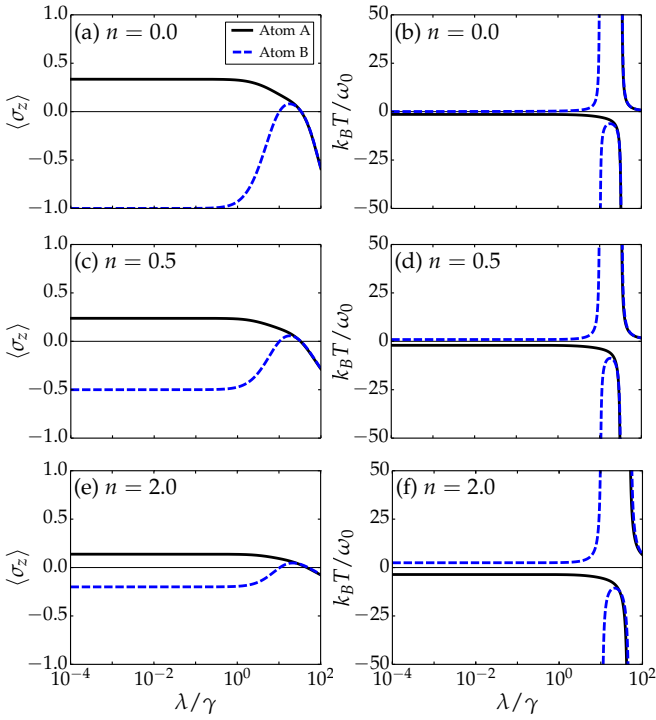


Figure IV.5: Scaled average energy  $\langle \sigma_z \rangle$  versus cooperativity, Figs. (a,c,e), and scaled effective temperature  $k_B T / \omega_0$  versus cooperativity, Figs. (b,d,f), for  $k = 2$ . The environment thermal photon averages are  $n = 0.0, 0.5$ , and  $2$ , respectively. Curves for atom A (B) is indicated by solid black (blue dashed) line. Here we used  $g_k = \sqrt{10}\gamma$  and  $\gamma = \gamma_A = \gamma_B = \kappa$ .

versus the environment thermal photon average  $n$  for the models  $k = 0, 1, 2, 3$ . It is to be noted that when  $k = 0$  Figs. (V.1)(a,b), the populations of the atoms A and B are not inverted, and thus we have the *conventional* (positive temperatures) CBH: by increasing its environment temperature, its internal energies, and therefore its effective temperature, is diminished. On the other hand, unconventional cooling by heating can occur for  $k \neq 0$ . Indeed, for  $k = 1$ , Figs. (V.1)(c,d), show that both atom B, with positive temperature, and atom A, with negative temperature [34], cool down by decreasing its internal energy when their environments are heated up. This effect is saturated near  $n \sim 0.5$  for the atom B, which has positive temperature, see Figs. (V.1)(c,d). This effect can be better appreciated by thinking in the opposite manner, i.e. in the *heating by cooling*: if the whole environment is cooled down, no matter if the atoms are with negative or positive temperatures, both atoms always heat up. This is a remarkable result, since, as emphasized above, it is usually expected that the energy flux between two systems with opposite signs to temperatures is from the one with negative to that with positive temperature, no matter as high the positive temperature is. On the other hand, the internal energy of atom A, and hence its temperature (solid black line), always de-

creases, as expected for systems with negative temperatures. Actually, energy flux between two systems is expected to be always from the one with negative to that with positive temperature [17–20].

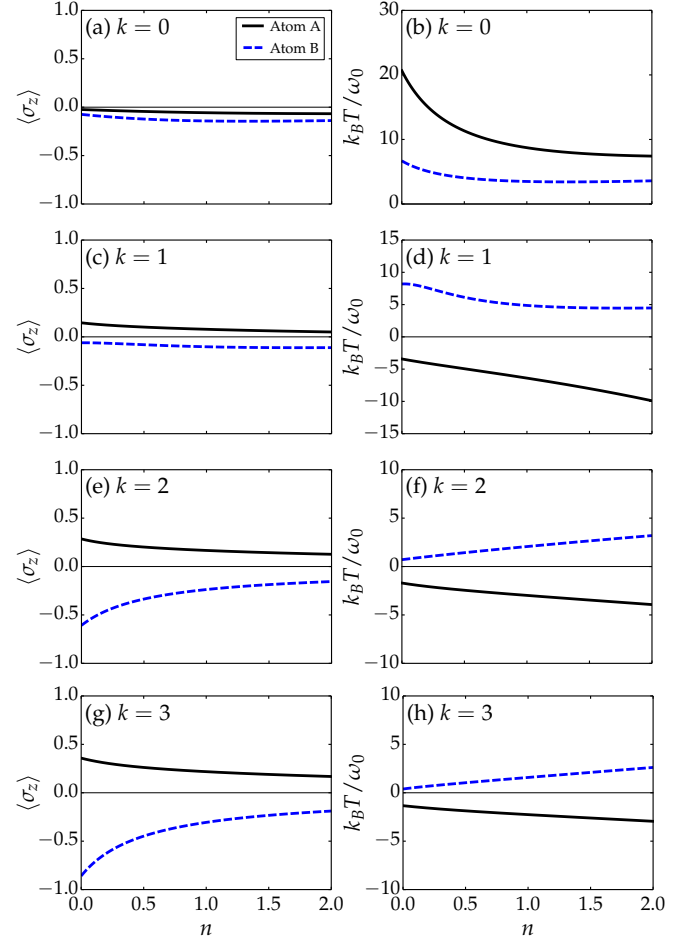


Figure V.1: The atom scaled average energy  $\langle \sigma_z \rangle$  and its scaled effective temperature  $k_B T / \omega_0$  versus the environment thermal photon average  $n$  for the models  $k = 0, 1, 2, 3$  and atoms A (solid black line) and B (blue dashed line). Except by  $k = 0$ , all the other models present negative temperature for atom A (solid black line). Here we used  $g_k = \sqrt{10}\gamma$  and  $\lambda = 3\gamma$ .

It is interesting to note that for  $k = 2$  and  $k = 3$ , Figs. (V.1)(e,f) and Figs. (V.1)(g,h), respectively, the CBH occurs only for atom A: by increasing the environment temperature, atom B (with positive temperature) heats up, while atom A (with negative temperature) cools down.

## VI. CONCLUSION

We have proposed an experimentally feasible platform to study systems capable to display population inversion in its steady state, and thus, presenting Boltzmann negative temperatures. Our platform includes i)

one qubit and a bosonic mode coupled through an effective Hamiltonian, the so-called anti-Jaynes-Cummings model (AJCM). The bosonic mode can be traced out to focus the attention on the qubit, which can display negative temperatures for a wide range of the cooperativity parameter, and ii) the previous system in i) plus another qubit, which is coupled to the first TL system through a natural Hamiltonian model, such as that stemming from collisions. Using our platform as a theoretical tool, we were able to study a variety of phenomena, such as the thermalization for two qubits when one or both of them presents negative temperature, the control of negative temperatures through the cooperativity parameter, and also what we have called *unconventional cooling by heating*, which occurs when, decreasing (increasing) the temperatures of the whole environment, the temperatures of one or both the two qubits increases (decreases), even when the temperature of one qubit is negative. This is a striking result if we remember that systems with negative temperatures are expected to decrease its negative temperature as in contact with another system having positive temperatures. Our proposal can be nowadays engineered in several contexts, such as trapped ions [24, 27], cavity QED [28], nanomechanical resonator [29], among others [30–32].

We acknowledge financial support from the Brazilian agency CNPq, CAPES and FAPEG. This work was performed as part of the Brazilian National Institute of Science and Technology (INCT) for Quantum Information (Grant No. 465469/2014-0). C.J.V.-B. acknowledges support from Brazilian agencies No. 2013/04162-5 Sao Paulo Research Foundation (FAPESP) and from CNPq (Grant No. 308860/2015-2).

- 
- [1] E. M. Purcell and R. V. Pound, Phys. Rev. 81, 279 (1951).  
 [2] N. F. Ramsey, Phys. Rev. 103, 20 (1956).  
 [3] R. J. Tykodi, Am. J. Phys. 43, 271 (1975).  
 [4] A.-M. Tremblay, Am. J. Phys. 44, 994 (1976).  
 [5] R. J. Tykodi, Am. J. Phys. 44, 997 (1976).  
 [6] A. Danielian, Am. J. Phys. 44, 995 (1976).  
 [7] P. T. Landsberg, J. Phys. A: Math. Gen. 10, 1773 (1977).  
 [8] R. J. Tykodi, Am. J. Phys. 46, 354 (1978).  
 [9] V. Berdichevsky, I. Kunin and F. Hussain, Phys. Rev. A 43, 2050 (1991).  
 [10] A. Rapp, S. Mandt and A. Rosch, Phys. Rev. Lett. 105, 220405 (2010).  
 [11] A. P. Mosk, Phys. Rev. Lett. 95, 040403 (2005).  
 [12] S. Braun, et al., Science 339, 52 (2013). [14] V. Romero-Rochn, Phys. Rev. E 88, 022144 (2013).  
 [13] [7] Sokolov, I.M. Thermodynamics: not hotter than hot. Nature Physics 10, 7-8 (2014).  
 [14] Jörn Dunkel and Stefan Hilbert, Nature Physics 10, 67–72 (2014) doi:10.1038/nphys2815  
 [15] Stefan Hilbert, Peter Hänggi, and Jörn Dunkel, Phys. Rev. E 90, 062116 (2014).  
 [16] Michele Campisi, Phys. Rev. E 91, 052147 (2015).  
 [17] D. Frenkel and P. B. Warren, American Journal of Physics, Volume 83, Issue 2, p.163-170  
 [18] Dragoş-Victor Anghel, EPJ Web of Conferences 108, 02007 (2016).  
 [19] Jose M. G. Vilar and J. Miguel Rubi, The Journal of Chemical Physics 140, 201101 (2014)  
 [20] Buonsante, Pierfrancesco; Franzosi, Roberto; Smerzi, Augusto, Annals of Physics, Volume 375, p. 414-434 (2016).  
 [21] ] F. O. Prado, N. G. de Almeida, M. H. Y. Moussa, and C. J. Villas-Boas, Phys. Rev. A 73, 043803 (2006)  
 [22] R. M. Serra, C. J. Villas-Boas, N. G. de Almeida, and M. H. Y. Moussa, *ibid.* 71, 045802 (2005).  
 [23] F. O. Prado, E. I. Duzzioni, M. H. Y. Moussa, N. G. de Almeida, and C. J. Villas-Bôas, Phys. Rev. Lett. 102, 073008 (2009).  
 [24] D. Leibfried et al., Rev. Mod. Phys. 75, 281 (2003).  
 [25] D. Z. Rossatto, A. R. de Almeida, T. Werlang, C. J. Villas-Boas, and N. G. de Almeida Phys. Rev. A 86, 035802 (2012).  
 [26] W. Vogel and R. L. de Matos Filho, Phys. Rev. A 52, 4214 (1995).  
 [27] J. F. Poyatos *et al.*, Phys. Rev. Lett. 77, 4728 (1996).  
 [28] W. Rosado, G.D. de Moraes Neto, F.O. Prado, and M.H.Y. Moussa, Journal of Modern Optics Vol. 62 , Iss. 19 (2015).  
 [29] Fei Xue, Ling Zhong, Yong Li, and C. P. Sun, Phys. Rev B 75, 033407 (2007)  
 [30] P. W. H. Pinkse, T. Fischer, P. Maunz, and G. Rempe, Nature 404, 365 (2000).  
 [31] J. McKeever, A. Boca, A. D. Boozer, J. R. Buck, and H. J. Kimble, Nature 425, 268 (2003).  
 [32] H. G. Barros, A. Stute, T. E. Northup, C. Russo, P. O. Schmidt, and R. Blatt, New J. Phys. 11, 103004 (2009).  
 [33] S. M. Tan, J. Opt. B 1, 424 (1999).  
 [34] Boltzmann temperatures scale from cold to hot according to  $+0K, \dots, +300K, \dots, +\infty K, -\infty K, \dots, -300K, \dots, -0K$ .  
 [35] Actually, *hotter than hot* is a criticism against negative temperatures, see Ref. [13].  
 [36] Shi-Biao Zheng, and Guang-Can Guo, Phys. Rev. Lett. 85, 2392 (2000).  
 [37] Loris Ferrari, arXiv:1501.04566.  
 [38] C. J. Hood, T. W. Lynn, A. C. Doherty, A. S. Parkins, and H. J. Kimble, Science 287, 1447 (2000).